Accepted Manuscript

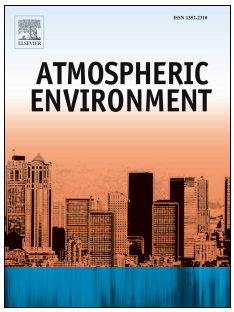

The impact of biomass burning on total suspended particulate matter in the southeastern Tibetan Plateau

Chong-Shu Zhu, Jun-Ji Cao, Zhi-Sheng Zhang, Sui-Xin Liu, Jia-Mao Zhou, Ping Wang, Jun Tao, Ting Zhang, Xiao-Li Su, Qi-Yuan Wang, Ning-Ning Zhang

PII: S1352-2310(18)30577-6

DOI: 10.1016/j.atmosenv.2018.08.056

Reference: AEA 16224

To appear in: *Atmospheric Environment*

Received Date: 23 April 2018

Revised Date: 8 August 2018

Accepted Date: 28 August 2018

Please cite this article as: Zhu, C.-S., Cao, J.-J., Zhang, Z.-S., Liu, S.-X., Zhou, J.-M., Wang, P., Tao, J., Zhang, T., Su, X.-L., Wang, Q.-Y., Zhang, N.-N., The impact of biomass burning on total suspended particulate matter in the southeastern Tibetan Plateau, *Atmospheric Environment* (2018), doi: 10.1016/j.atmosenv.2018.08.056.

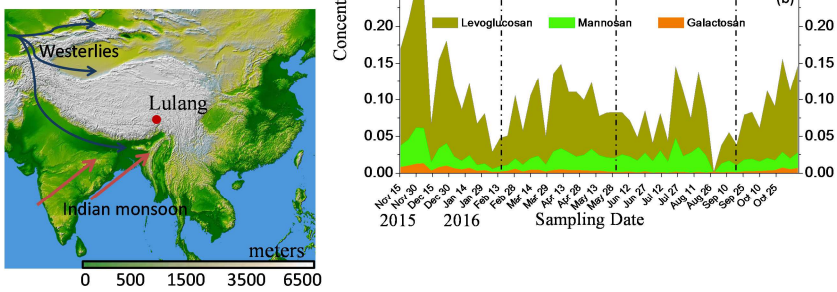

The impact of biomass burning on total suspended particulate matter in the southeastern Tibetan Plateau

Chong-Shu Zhu[1*], Jun-Ji Cao[1], Zhi-Sheng Zhang[2], Sui-Xin Liu[1], Jia-Mao Zhou[1], Ping Wang[3], Jun Tao[2], Ting Zhang[1], Xiao-Li Su[1], Qi-Yuan Wang[1], Ning-Ning Zhang[1]

[1]*Key Laboratory of Aerosol Chemistry and Physics, SKLLQG, Institute of Earth Environment, Chinese Academy of Sciences, Xi'an 710061, China*

[2]*South China Institute of Environmental Sciences, Ministry of Environmental Protection, Guangzhou 510000, China*

[3]*School of Science and Technology, Hainan Tropical Ocean University, Sanya 572022, China*

[*] Corresponding author. Postal address: Institute of Earth Environment, Chinese Academy of Sciences, No. 97 Yan xiang Road, Yan-ta Zone, Xi'an 710061, Shaanxi, China. E-mail: chongshu@ieecas.cn Tel: 86-29-6233-6272, Fax: 86-29-6233-6234

Abstract

To investigate the impact of biomass burning (BB) emissions on total suspended particulate (TSP) in the southeastern Tibetan Plateau (TP), BB tracers (including levoglucosan, mannosan, and galactosan) were measured at Lulang (a remote site, ~3300 m above sea level) during the period 2015–2016. The concentrations of levoglucosan and mannosan showed large variability of more than 8-fold (range: 0.029–0.253 μg m^{-3}) and 6-fold (range: 0.01–0.061 μg m^{-3}), respectively. The highest seasonal average concentrations of levoglucosan (0.131 ± 0.073 μg m^{-3}) and mannosan (0.028 ± 0.019 μg m^{-3}) were observed during the winter season. The BB contributions to the TSP organic carbon (OC) and TSP mass were estimated with positive matrix factorization (PMF) by using BB tracers, inorganic ions, elements, OC, and EC. The BB contributions to the TSP OC and TSP mass were quite substantial in winter with 26% and 14%, respectively. The results evidenced a major contribution of BB to the aerosol OC during winter season. Major potential source distributions of BB were identified, which included the pollution bands along the Indo-Gangetic Plain, the Yarlung Tsangpo River Valley and the interior of the TP. In addition to the long-range transport of BB, the sources of anthropogenic emissions (residential BB for cooking and heating) in the TP may be an important contributor. The results facilitated understanding of the characteristics and effects of BB in the TP.

Keywords: Levoglucosan; Biomass burning; Tibetan Plateau

1. Introduction

The Tibetan Plateau (TP) plays important roles in global climate and environment (Ramanathan et al., 2005, 2007; Yao et al., 2012). The TP glaciers with seasonal and permanent snow cover affect the water supply of some Asian rivers. This has had a significant impact on water resources for billions of local habitants in Asia (Ming et al., 2013; Xu et al., 2009a). Previous studies found that carbonaceous aerosols can reduce snow albedo, and are considered as important contributors to the accelerating melting of Tibetan glaciers (Ming et al., 2013; Wang et al., 2015a; Xu et al., 2009a), which is mainly from biomass and fossil fuel combustion emissions (Wang et al., 2015b; Xu et al., 2009b; Xu et al., 2012; You et al., 2016).

Biomass burning (BB) aerosols are considered to be a major cause of the South Asia Brown Clouds (Gustafsson et al., 2009; Engling and Gelencser, 2010). The BB pollutants from the Indo-Gangetic Plain and South Asia can be transported to the upper troposphere by thermal convection processes (Kahn et al., 2008; Vadrevu et al., 2012), where they can be transported to the TP (Cong et al., 2015; Zhao et al., 2017). Therefore, it is rather important and necessary to obtain insight into the impact of BB aerosol in the above-mentioned vulnerable regions.

Levoglucosan is considered as a highly specific tracer for BB aerosols because it can normally remain stable for several days under most atmospheric conditions during the transport process (Mochida, 2003; Giannoni et al., 2012; Maenhaut et al., 2012; Cong et al., 2015; Zangrando et al., 2016). Mannosan and galactosan can also be used as BB tracers (Bernardoni et al., 2011; Maenhaut et al., 2012; Sang et al., 2013). The use of levoglucosan as BB tracer has been preferred to the conventional water soluble potassium, since potassium has other sources (Caseiro et al., 2009; Duan et al., 2004). The study on the spatio-temporal characteristics of BB aerosols over the TP is still limited due to its extremely high elevation and its harsh natural environment.

In this study, the variations of carbonaceous fractions and BB tracers (including levoglucosan, mannosan, and galactosan) were investigated at a representative site (Lulang, influenced by the Indian monsoon and westerly winds) in the southeastern TP. The selection of the site could provide important information to better understand

the impact of air pollutants from the south of the Himalayas and the interior of the TP. The BB contributions to total suspended particulate (TSP) mass and organic carbon (OC) in the region were evaluated. Based on the BB tracer of levoglucosan, the major potential source distributions of BB were obtained during the sampling period.

2. Methods

2.1. Aerosol Sampling

Figure 1 shows the sampling site location at Lulang (94.73°E, 29.76°N, 3326 m a.s.l.) in the southeastern margin of the TP. In terms of meteorological conditions, Lulang exhibits the typical characteristics of the Indo-Gangetic Plain climate with wet monsoon season (June–September), dry winter season (December–February), pre-monsoon season (March–May) and post-monsoon season (October–November). The sampling was performed on the roof of a tower (10 m above the ground) in the premises of the South-East Tibetan plateau Station for integrated observation and research of alpine environment, Chinese Academy of Sciences (CAS).

TSP samples were collected on a weekly basis at 17 L/min with a custom-built sampler on 47 mm Whatman quartz–fiber filters (QM/A) from November 2015 to November 2016. Field blank filters were also collected periodically. Quartz–fiber filters were pre-heated at 900 □ for 3 hours to remove the residual carbon. The samples were stored immediately in a refrigerator at about –20 □ to prevent the evaporation of volatile components after sampling.

Figure 1

2.2. Measurement of OC and EC

The quartz microfibre filters were analyzed for carbon fractions using a DRI Model 2001 Thermal/Optical Carbon Analyzer (Atmoslytic Inc., Calabasas, CA, USA). Carbon fractions were obtained following the IMPROVE-A (Interagency Monitoring of Protected Visual Environments) thermal/optical reflectance protocol (Chow et al., 2007). The method reports data for four OC fractions in a helium atmosphere (OC1,

OC2, OC3, and OC4 at 140 ^{o}C, 280 ^{o}C, 480 ^{o}C, and 580 ^{o}C, respectively), a pyrolyzed carbon fraction (OP), and three elemental carbon (EC) fractions in a 2% oxygen/98% helium atmosphere (EC1, EC2, and EC3 at 580 ^{o}C, 740 ^{o}C, and 840 ^{o}C, respectively). OC and EC were defined as OC1+OC2+OC3+OC4+OP and EC1+EC2+EC3-OP, respectively. Field blank filters were also analyzed in order to correct the results. The detailed procedures of quality assurance/quality control (QA/QC) have been reported elsewhere (Cao et al., 2003; Chow et al., 2011).

2.3. Measurement of levoglucosan, mannosan, and galactosan

The TSP samples were analyzed for levoglucosan, mannosan, and galactosan by using high-performance anion exchange chromatography with pulsed amperometric detection (HPAEC-PAD). A detailed description of the analytical method has been reported elsewhere (Engling et al., 2006). The HPAEC-PAD method has been developed and validated for determination of atmospherically relevant sugar alcohols, monosaccharides, and monosaccharide anhydrides (Zhang et al., 2013). The instrumental limit of detection was determined as the peak height at least three times the signal to noise ratio. The HPAEC-PAD method detection limits were 4 ppb for levoglucosan and 2 ppb for mannosan and galactosan, respectively.

2.4. Measurement of inorganic ions and elements

Four anions (SO_4^{2-}, NO_3^-, Cl^-, and F^-) and five cations (Na^+, NH_4^+, K^+, Mg^{2+}, and Ca^{2+}) in aqueous extracts of the filters were analyzed using ion chromatography (IC). The elemental concentrations were determined using energy-dispersive x-ray fluorescence (ED-XRF) spectrometry, which provides a rapid method for the analysis of trace and major elements in samples. A detailed description of the detection limits and methodology for the analyses can be found elsewhere (Cao et al., 2012).

3. Results and discussion

3.1. Variations of TSP, OC, and EC mass

Figure 2a shows the variations of TSP, OC, and EC mass at the Lulang site. Compared to OC and EC, the weekly TSP concentrations showed larger variations during the sampling period. TSP concentrations varied over 5.8-fold from a low of 6.39 to 37.28 μg m^{-3}, and OC varied over 3.2-fold from 1.11 to 3.52 μg m^{-3}. The pattern indicated that there were important seasonal contributors to TSP besides of carbonaceous fraction.

Annual and seasonal average TSP, OC, and EC mass concentrations were reported in Table 1 during the sampling period. TSP levels were higher in pre-monsoon (mean value 19.1 ± 8.3 μg m^{-3}), with respect to winter (16.7 ± 4.4 μg m^{-3}), monsoon (12.5 ± 5.5 μg m^{-3}), and post-monsoon (13.6 ± 2.7 μg m^{-3}), respectively. The highest OC concentrations were observed in monsoon season (2.52 ± 0.61 μg m^{-3}), followed by winter (2.1 ± 0.44 μg m^{-3}), pre-monsoon (1.98 ± 0.58 μg m^{-3}), and post-monsoon (1.88 ± 0.20 μg m^{-3}). The annual concentrations of TSP, OC, and EC mass were 15.2 ± 6.4 μg m^{-3}, 2.1 ± 0.64 μg m^{-3}, and 0.74 ± 0.22 μg m^{-3}, respectively. The variations of the EC mass showed small difference during the sampling period (Figure 2a).

Table 1

3.2. The variations of levoglucosan, mannosan, and galactosan

The concentrations of levoglucosan and mannosan showed large variability during the study period (Figure 2b). The weekly levoglucosan concentrations varied over 8.7-fold from 0.029 to 0.253 μg m^{-3}, and mannosan varied over 6-fold from 0.010 to 0.060 μg m^{-3}. Levoglucosan and mannosan exhibited a similar seasonal cycle, with the highest concentrations of 0.131 ± 0.073 μg m^{-3} and 0.028 ± 0.019 μg m^{-3} in winter, respectively. The lowest values of levoglucosan (0.072 ± 0.038 μg m^{-3}) and mannosan (0.021 ± 0.005 μg m^{-3}) were observed during the monsoon and post-monsoon, respectively. Comparable seasonal levels of galactosan were found in the range of 0.001 ± 0.001 μg m^{-3} (monsoon) to 0.007 ± 0.004 μg m^{-3} (winter) (Table 1). It is to be noted that the galactosan concentrations of some monsoon samples were lower than the instrumental limit of detection. The annual average concentrations for

156 levoglucosan, mannosan, and galactosan in the present study were 0.097 ± 0.051 μg
157 m^{-3}, 0.023 ± 0.012 μg m^{-3}, and 0.004 ± 0.003 μg m^{-3}, respectively. The highest
158 levels were noted in winter for the BB tracers, thus indicating that BB is most intense
159 in the coldest season of the year.

160 The concentrations of the TSP, OC and EC mass, and levoglucosan at Lulang were
161 lower than those measured in the southern area of the TP. For example, higher levels
162 of TSP (196 ± 132 μg m^{-3}), OC (32.8 ± 21.5 μg m^{-3}), EC (5.95 ± 2.70 μg m^{-3}), and
163 levoglucosan (0.73 ± 1.04 μg m^{-3}) were obtained at Lumbini, Nepal (Wan et al.,
164 2017). The concentrations of levoglucosan at Lulang were much lower than at
165 BB-influenced sites in India with values reported for New Delhi (1.98 μg m^{-3}),
166 Raipur (2.18 μg m^{-3}) and Rajim (2.26 μg m^{-3}), respectively (Deshmukh et al., 2016;
167 Li et al., 2014; Nirmalkar et al., 2015). The latter sites in Nepal and India were close
168 to anthropogenic sources and were possibly influenced by local agricultural burning
169 or forest fires.

170

171 Figure 2

172

173 *3.3. Source identification and apportionment by PMF*

174 PMF (positive matrix factorization) is a receptor model, which is a mathematical
175 approach for quantifying the contributions of sources to samples based on the
176 chemical composition or source fingerprints (Paatero, 1997). PMF 5.0 was used for
177 the current analysis.

178 The source profiles for the base model 7-factor solution and the average percentage
179 apportionments of the various species to the factors are shown in Figure 3.
180 Considering the key species, the source association of the 7 factors seemed overall
181 quite logical. Factor 1 was dominated by OC, EC, Zn, Mn, and Fe, and is best
182 interpreted as combustion aerosol and traffic-related emissions. The second PMF
183 factor had high loadings for OC, Na^+, K^+, Cl^-, and Mg^{2+}, and this factor can most
184 readily be explained as a combination of secondary organic carbon and sea salt.

Factor 1 and factor 2 accounted for 14.9% and 14.4% of TSP mass, respectively. The levels of NO_3^-, Cl^-, Ca^{2+} and Mg^{2+} in the profiles of the third factor were very high, and this can be attributed to the formation of secondary nitrate. Factor 4 was characterized by high loadings of elements such as Ba, Fe, Ca, Ti, and Mn, and this factor can most readily be explained by road dust and fugitive dust. Factor 3 and factor 4 accounted for 13.6% and 17.7% of TSP mass, respectively. Factor 5 was determined to be representative of secondary sulfate since SO_4^{2-} and NH_4^+ were highly loaded on this factor. Factor 6 was enriched in crustal elements (e.g., Ca, Fe, Ti, K, Mg^{2+}, Ca^{2+}, and Cl^-), and this factor is most likely associated with mineral aerosol. This factor was the largest contributor to TSP mass, accounting for 25.9% during the sampling periods. The results suggest that mineral aerosol is the most important source for the TSP mass at Lulang. Factor 7 appeared to represent BB. Loadings on this profile were high for levoglucosan, galactosan, OC, and EC. This source accounted for 7.9% of TSP mass for the sampling period.

Figure 3

3.4. Contributions from BB to the TSP OC and TSP mass

Figure 4 shows the time series of the percentages TSP OC and TSP mass from BB at Lulang. The patterns in both figures were fairly similar to that observed in Figure 2 for the time series of levoglucosan. The seasonal ranges of 3–43%, 6–30%, 5–24%, and 8–34% for % TSP OC from BB were obtained in winter, pre-monsoon, monsoon, and post-monsoon, respectively, whereas those for the % TSP mass from BB were in the ranges of 3–22%, 3–16%, 4–23%, and 4–21% for winter, pre-monsoon, monsoon, and post-monsoon, respectively. The percentage contributions from BB to the TSP OC and TSP mass showed a clear seasonal character. The seasonal averages for the % TSP OC from BB were 26%, 17%, 12%, and 17% for winter, pre-monsoon, monsoon, and post-monsoon, respectively, while those for the % TSP mass were 14%, 8%, 10%, and 10% for winter, pre-monsoon, monsoon, and post-monsoon, respectively. The

average BB contributions were quite substantial in winter for the TSP OC and TSP mass. The lowest percentages were obtained for the % TSP mass in pre-monsoon and the % TSP OC mass in monsoon, respectively. The annual contributions from BB to the TSP OC and TSP mass were 18% and 11% during the sampling period, respectively. The sharp variations clearly illustrated the impact from BB (including local emissions and long-range atmospheric transport) on the TSP OC and TSP mass, especially in winter.

The contributions of BB to the TSP mass in the present study were comparable to those of 14% for Swiss sites (Gianini et al., 2013), while the values were much lower than those of 37% (annual average) and 50% (during winter) of the PM_{10} mass for an urban background site in northern Tuscany (Nava et al., 2015). The winter contributions of BB to the TSP OC mass in the present study were comparable to those of PM_{10} aerosol in Flanders, Belgium (Maenhaut et al., 2016), while the levels were higher than those of 6.5-11% in Hong Kong (Sang et al., 2011), and 16-28% in Hainan (Zhang et al., 2012), respectively.

Figure 4

From scatter plots of the PMF-derived BB TSP OC mass and TSP mass versus levoglucosan, we can arrive at conversion factors of 3.6 (R= 0.93) and 14.4 (R= 0.93), respectively (Figure 5). The conversion factors were comparable to those in Flanders, Belgium (Maenhaut et al., 2012). The values estimated in the present study were much lower than the PMF-derived conversion factors of 9.7 and 22.6 for OC and PM_{10}, respectively (Maenhaut et al., 2016). Larger factors for particulates were reported by some previous studies in Europe, with values reported for The Netherlands, Helsinki (24 ± 9) and Switzerland (ranging from 15.3 to 29), respectively (Kos and Weijers, 2009; Saarnio et al., 2012; Gianini et al., 2013). The differences can be partly attributed to the variations in the type of biofuel and the burning conditions. It is recommended to use the conversion factors for deriving the contribution from BB when making use of levoglucosan as single marker at the

remote site.

Figure 5

3.5. The transport and potential source regions of biomass burning

To better understand the transport mechanism and potential source areas of BB, seasonal distributions of fire hot spots were acquired from MODIS observations (https://firms.modaps.eosdis.nasa.gov/). In addition, to assess the impact of regional transported air pollutants in the Lulang region, three-day backward air-mass trajectories corresponding to each sampling date were calculated using the HYSPLIT model (Draxler and Rolph, 2012). The potential source contribution function (PSCF) has been used to identify the potential locations of regional pollution sources (Polissar et al., 1999; Hsu et al., 2003). In this study, the PSCF values were calculated by using levoglucosan and three-day back trajectories arriving at Lulang at 1000 LST (local standard time) during the sampling period.

Figure 6 shows that the pre-monsoon period is the major fire season in the lowland of the southern Himalayas. The fire spots were seen to be more concentrated in areas in India and Nepal compared with the interior of the TP. A previous study also reported that there were intense agricultural burning activities and forest fires along the southern Himalayan foothills and the Northern Indo-Gangetic Plain in pre-monsoon. The pollutants can enter the TP by the valleys in the eastern Himalayan section (Cong et al., 2015).

Figure 6.

Figure 7 shows the trajectories that were calculated from the individual three-day backward trajectories in four seasons. For discussion purposes, we arbitrarily defined a trajectory as “polluted” (brown color) when the levoglucosan concentrations exceed the seasonal geometric mean concentration plus one geometric standard deviation of the mean. Of all backward trajectories included in the analysis for winter, ~21% of

those were considered polluted. The average levoglucosan concentration for these polluted trajectories was 0.24 μg m^{-3}. The air masses in the pre-monsoon cluster originated from northern India and over central Tibet. The percent contribution of ~20% for the trajectories in the pre-monsoon cluster were classified as polluted and had a mean value of 0.14 μg m^{-3}. The air masses grouped into the monsoon cluster were from the northeastern India with a polluted trajectories contribution of 19%, and the average levoglucosan mass concentration of the polluted trajectories was 0.13 μg m^{-3}. The air masses in post-monsoon originated from the Indo-Gangetic Plain and then moved across northeastern India and to the southeast of Tibet before arriving at Lulang. The average levoglucosan concentration for these polluted trajectories was 0.15 μg m^{-3}. The percentage of the polluted trajectories assigned to this cluster was ~25%.

In the winter and pre-monsoon seasons, strong westerlies pass through Nepal, northwest India and Pakistan as well as the interior area of Tibet. In the monsoon and post-monsoon season, air masses are derived from Bangladesh and northeast India and bring moisture that originates from the Bay of Bengal. The highest levoglucosan level for the "polluted trajectory" was found in winter season. In addition to natural fire emissions, anthropogenic emissions (residential BB for cooking and heating) may be important BB sources in the TP.

Figure 7

Figure 8 shows the PSCF plots for the major BB source areas, in which PSCF values were displayed with regard to color scale. The important potential source regions (PS1, PS2, PS3, and PS4), were likely located in the high PSCF value regions. PS1 covered the Yarlung Tsangpo River Valley and local areas. Air pollutants can be transported through the Yarlung Tsangpo River Valley from the Indo-Gangetic Plain and Bangladesh to the site. PS2 covered the interior of the TP from the western area (including some villages and cities). Considering the scarce distribution of fire hot spots in the area, the results for PS1 and PS2 suggest the influence of residential BB

from cooking and heating. PS3 and PS4 included the obvious pollution bands along the Indo-Gangetic Plain, which was consistent with the fire hot spots area in pre-monsoon and winter. The pollution bands covered the northern area of India, western area of Nepal and the area of Katmandu. The prevailing wind direction around the southeastern margin of the TP was southerly, and the pollutants in the pollution bands could be transported to Lulang along the valley of the Yarlung Tsangpo River as a "leaking wall" (Cao et al., 2011). The air mass transport from the Indo-Gangetic Plain region to the TP has also been proposed to follow specific pathways (Cong et al., 2015; Zhao et al., 2017).

Figure 8

Conclusions

In the present study, the variations of carbonaceous fractions and BB tracers (including levoglucosan, mannosan, and galactosan) were investigated for TSP at Lulang in the southeastern margin of the TP. The results provided a better understanding on the magnitude of levoglucosan, mannosan, and galactosan. The seasonal variation patterns of BB tracers are different from TSP and OC. The highest seasonal concentrations for TSP, OC, and BB tracers (levoglucosan and mannosan) were observed during pre-monsoon, monsoon, and winter seasons, respectively. The annual contributions from BB to the TSP OC and TSP mass were 18% and 11%, and were quite substantial in winter with 26% and 14%, respectively. The results indicated that BB is an important contributor, especially in winter. The seasonal BB pollutant transport and major potential source distributions of BB were identified, which included the pollution bands along the Indo-Gangetic Plain, the Yarlung Tsangpo River Valley and the interior of the TP. In addition to long-range transport of BB aerosol, anthropogenic BB aerosol from cooking and heating may be an important contributor in the TP. The results can facilitate the knowledge for the characteristics and effects of BB in the TP and guide policy actions aimed to effectively mitigate emissions.

Acknowledgements

This study was supported by the National Natural Science Foundation of China (41771518). The authors are grateful to the South-East Tibetan plateau Station for integrated observation and research of alpine environment, CAS for the assistance with filed sampling. The data of fire hot spots are available on the website (https://firms.modaps.eosdis.nasa.gov/). We also thank two anonymous reviewers for their valuable comments.

References

Bernardoni, V., Vecchi, R., Valli, G., Piazzalunga, A., Fermo, P., 2011. PM10 source apportionment in Milan (Italy) using time-resolved data. Science of the Total Environment 409, 4788–4795.

Cao, J.J., Tie, X.X., Xu, B.Q., Zhao, Z.Z., Zhu, C.S., Li, G.H., Liu, S.X., 2011. Measuring and modeling black carbon (BC) contamination in the SE Tibetan Plateau. Journal of Atmospheric Chemistry 67, 45–60.

Cao, J.J., Lee, S.C., Ho, K.F., Zhang, X.Y., Zou, S.C., Fung, K., Chow, J.C., Watson, J.G., 2003. Characteristics of carbonaceous aerosol in Pearl River Delta Region, China during 2001 winter period. Atmospheric Environment 37, 1451–1460.

Cao, J.J., Shen, Z.X., Chow, J.C., Watson, J.G., Lee, S.C., Tie, X.X., Ho, K.F., Wang, G.H., Han, Y.M., 2012. Winter and summer $PM_{2.5}$ chemical compositions in fourteen Chinese cities. Journal of the Air & Waste Management Association 62, 1214–1226.

Caseiro, A., Bauer, H., Schmidl, C., Pio, C.A., Puxbaum, H., 2009. Wood burning impact on PM10 in three Austrian regions. Atmospheric Environment 43, 2186–2195.

Chow, J.C., Watson, J.G., Chen, L.W.A., Chang, M.C.O., Robinson, N.F., Trimble, D., Kohl, S., 2007. The IMPROVE_A temperature protocol for thermal/optical carbon analysis: maintaining consistency with a long-term database. Journal of the Air & Waste Management Association 57, 1014–1023.

364 Chow, J.C., Watson, J.G., Robles, J., Wang, X., Chen, L.W., Trimble, D.L., Kohl,
365 S.D., Tropp, R.J., Fung, K.K., 2011. Quality assurance and quality control for
366 thermal/optical analysis of aerosol samples for organic and elemental carbon.
367 Analytical and bioanalytical chemistry 401, 3141–3152.
368 Cong, Z.Y., Kawamura, K., Kang, S., Fu, P., 2015. Penetration of biomass-burning
369 emissions from South Asia through the Himalayas: new insights from
370 atmospheric organic acids. Scientific reports 5, 9580.
371 Deshmukh, D.K., Kawamura, K., Deb, M.K., 2016. Dicarboxylic acids,
372 omega-oxocarboxylic acids, alpha-dicarbonyls, WSOC, OC, EC, and inorganic
373 ions in wintertime size-segregated aerosols from central India: Sources and
374 formation processes. Chemosphere 161, 27–42.
375 Draxler, R.R. and Rolph, G.D., 2012. HYSPLIT (HYbrid Single-Particle Lagrangian
376 Integrated Trajectory) Model access via NOAA ARL READY Website,
377 available at: http://ready.arl.noaa.gov/HYSPLIT.php, NOAA Air Resources
378 Laboratory, Silver Spring, MD.
379 Duan, F., Liu, X., Yu, T., Cachier, H., 2004. Identification and estimate of biomass
380 burning contribution to the urban aerosol organic carbon concentrations in
381 Beijing. Atmospheric Environment 38, 1275–1282.
382 Engling, G., Carrico, C.M., Kreidenweis, S.M., Collett Jr, J.L., Day, D.E., Malm,
383 W.C., Lincoln, E., Min Hao, W., Iinuma, Y., Herrmann, H., 2006. Determination
384 of levoglucosan in biomass combustion aerosol by high-performance
385 anion-exchange chromatography with pulsed amperometric detection.
386 Atmospheric Environment 40, 299–311.
387 Engling, G., Gelencser, A., 2010. Atmospheric brown clouds: from local air pollution
388 to climate change. Elements 6, 223–228.
389 Gianini, M.F.D., Piot, C., Herich, H., Besombes, J.L., Jaffrezo, J.L., Hueglin, C., 2013.
390 Source apportionment of PM10, organic carbon and elemental carbon at Swiss
391 sites: an intercomparison of different approaches. Science of the Total
392 Environment 454–455, 99–108.
393 Giannoni, M., Martellini, T., Del Bubba, M., Gambaro, A., Zangrando, R., Chiari, M.,

Lepri, L., Cincinelli, A., 2012. The use of levoglucosan for tracing biomass burning in PM2.5 samples in Tuscany (Italy). Environmental Pollution 167, 7–15.

Gustafsson, O., Krusa, M., Zencak, Z., Sheesley, R.J., Granat, L., Engstrom, E., Praveen, P.S., Rao, P.S., Leck, C., Rodhe, H., 2009. Brown clouds over South Asia: biomass or fossil fuel combustion? Science 323, 495–498.

Hsu, Y.K., Holsen, T.M. and Hopke, P.K., 2003. Comparison of hybrid receptor models to locate PCB sources in Chicago. Atmospheric Environment 37, 545–562.

Kahn, R.A., Chen, Y., Nelson, D.L., Leung, F.Y., Li, Q., Diner, D.J., Logan, J.A., 2008. Wildfire smoke injection heights: Two perspectives from space. Geophysical Research Letters 35, 228–236.

Kos, G.P.A., Weijers, E.P., 2009. De bijdrage van houtverbranding aan PM10 en PM2.5 tijdens een winterperiode in Schoorl (in Dutch). ECN-E–09-083. Energieonderzoek Centrum, Nederland (November).

Li, J.J., Wang, G.H., Aggarwal, S.G., Huang, Y., Ren, Y.Q., Zhou, B.H., Singh, K., Gupta, P.K., Cao, J.J., Zhang, R., 2014. Comparison of abundances, compositions and sources of elements, inorganic ions and organic compounds in atmospheric aerosols from Xi'an and New Delhi, two megacities in China and India. Science of the Total Environment 476–477, 485–495.

Maenhaut, W., Vermeylen, R., Claeys, M., Vercauteren, J., Matheeussen, C., Roekens, E., 2012. Assessment of the contribution from wood burning to the PM10 aerosol in Flanders, Belgium. Science of the Total Environment 437, 226–236.

Maenhaut, W., Vermeylen, R., Claeys, M., Vercauteren, J., Roekens, E., 2016. Sources of the PM10 aerosol in Flanders, Belgium, and re-assessment of the contribution from wood burning. Science of the Total Environment 562, 550–560.

Ming, J., Xiao, C., Du, Z., Yang, X., 2013. An overview of black carbon deposition in High Asia glaciers and its impacts on radiation balance. Advances in Water Resources 55, 80–87.

Mochida, M., 2003. Spatial distributions of oxygenated organic compounds (dicarboxylic acids, fatty acids, and levoglucosan) in marine aerosols over the western Pacific and off the coast of East Asia: Continental outflow of organic aerosols during the ACE-Asia campaign. Journal of Geophysical Research 108(D23), 8638, doi:10.1029/2002JD003249, 2003.

Nava, S., Lucarelli, F., Amato, F., Becagli, S., Calzolai, G., Chiari, M., Giannoni, M., Traversi, R., Udisti, R., 2015. Biomass burning contributions estimated by synergistic coupling of daily and hourly aerosol composition records. Science of the Total Environment 511, 11–20.

Nirmalkar, J., Deshmukh, D.K., Deb, M.K., Tsai, Y.I., Sopajaree, K., 2015. Mass loading and episodic variation of molecular markers in $PM_{2.5}$ aerosols over a rural area in eastern central India. Atmospheric Environment 117, 41–50.

Paatero, P., 1997. Least squares formulation of robust nonnegative factor analysis. Chemometrics and Intelligent Laboratory Systems 37, 15–35.

Polissar, A.V., Hopke, P.K., Paatero, P., Kaufmann, Y.J., Hall, D.K., Bodhaine, B.A., Dutton, E.G. and Harris, J.M., 1999. The aerosol at Barrow, Alaska: long-term trends and source locations. Atmospheric Environment 33, 2441–2458.

Ramanathan, V., Chung, C., Kim, D., Bettge, T., Buja, L., Kiehl, J.T., Washington, W.M., Fu, Q., Sikka, D.R., Wild, M., 2005. Atmospheric brown clouds: impacts on South Asian climate and hydrological cycle. Proceedings of the National Academy of Sciences of the United States of America 102, 5326–5333.

Ramanathan, V., Ramana, M.V., Roberts, G., Kim, D., Corrigan, C., Chung, C., Winker, D., 2007. Warming trends in Asia amplified by brown cloud solar absorption. Nature 448, 575–578.

Saarnio, K., Niemi, J. V., Saarikoski, S., Aurela, M., Timonen, H., Teinilä, K., Myllynen, M., Frey, A., Lamberg, H., Jokiniemi, J., and Hillamo, R., 2012. Using monosaccharide anhydrides to estimate the impact of wood combustion on fine particles in the Helsinki Metropolitan Area. Boreal Environment Research, 17, 163–183.

Sang, X.F., Zhang, Z.S., Chan, C.Y., Engling, G., 2013. Source categories and

454 contribution of biomass smoke to organic aerosol over the southeastern Tibetan
455 Plateau. Atmospheric Environment 78, 113–123.
456 Sang, X.F., Chan, C.Y., Engling, G., Chan, L.Y., Wang, X.M., Zhang, Y.N., Shi, S.,
457 Zhang, Z.S., Zhang, T., Hu, M., 2011. Levoglucosan enhancement in ambient
458 aerosol during springtime transport events of biomass burning smoke to
459 Southeast China. Tellus B: Chemical and Physical Meteorology 63, 129–139.
460 Vadrevu, K.P., Ellicott, E., Giglio, L., Badarinath, K.V.S., Vermote, E., Justice, C.,
461 Lau, W.K.M., 2012. Vegetation fires in the himalayan region-aerosol load, black
462 carbon emissions and smoke plume heights. Atmospheric Environment 47,
463 241–251.
464 Wan, X., Kang, S., Li, Q., Rupakheti, D., Zhang, Q., Guo, J., Chen, P., Tripathee, L.,
465 Rupakheti, M., Panday, A.K., Wang, W., Kawamura, K., Gao, S., Wu, G., Cong,
466 Z., 2017. Organic molecular tracers in the atmospheric aerosols from Lumbini,
467 Nepal, in the northern Indo-Gangetic Plain: influence of biomass burning.
468 Atmospheric Chemistry and Physics 17, 8867–8885.
469 Wang, M., Xu, B.Q., Cao, J.J., Tie, X.X., Wang, H., Zhang, R., Qian, Y., Rasch, P.J.,
470 Zhao, S., Wu, G., Zhao, H., Joswiak, D.R., Li, J., Xie, Y., 2015a. Carbonaceous
471 aerosols recorded in a southeastern Tibetan glacier: analysis of temporal
472 variations and model estimates of sources and radiative forcing. Atmospheric
473 Chemistry and Physics 15, 1191–1204.
474 Wang, M., Xu, B.Q., Kaspari, S.D., Gleixner, G., Schwab, V.F., Zhao, H., Wang, H.,
475 Yao, P., 2015b. Century-long record of black carbon in an ice core from the
476 Eastern Pamirs: Estimated contributions from biomass burning. Atmospheric
477 Environment 115, 79–88.
478 Xu, B.Q., Cao, J.J., Hansen, J., Yao, T.D., Joswia, D.R., Wang, N.L., Wu, G.J., Wang,
479 M., Zhao, H.B., Yang, W., Liu, X.Q., He, J.Q., 2009a. Black soot and the
480 survival of Tibetan glaciers. Proceedings of the National Academy of Sciences of
481 the United States of America 106, 22114–22118.
482 Xu, B.Q., Wang, M., Joswiak, D.R., Cao, J.J., Yao, T.D., Wu, G.J., Yang, W., Zhao,
483 H.B., 2009b. Deposition of anthropogenic aerosols in a southeastern Tibetan

glacier. Journal of Geophysical Research 114, D17209, doi:10.1029/2008JD011510.

Xu, B.Q., Cao, J.J., Joswiak, D.R., Liu, X., Zhao, H., He, J., 2012. Post-depositional enrichment of black soot in snow-pack and accelerated melting of Tibetan glaciers. Environmental Research Letters 7, 014022.

Yao, T.D., Thompson, L.G., Mosbrugger, V., Zhang, F., Ma, Y., Luo, T., Xu, B., Yang, X., Joswiak, D.R., Wang, W., Joswiak, M.E., Devkota, L.P., Tayal, S., Jilani, R., Fayziev, R., 2012. Third Pole Environment (TPE). Environmental Development 3, 52–64.

You, C., Xu, C., Xu, B.Q., Zhao, H.B., Song, L.L., 2016. Levoglucosan evidence for biomass burning records over Tibetan glaciers. Environmental Pollution 216, 173–181.

Zangrando, R., Barbaro, E., Vecchiato, M., Kehrwald, N.M., Barbante, C., Gambaro, A., 2016. Levoglucosan and phenols in Antarctic marine, coastal and plateau aerosols. Science of the Total Environment 544, 606–616.

Zhang, Y.N., Zhang, Z.S., Chan, C.Y., Engling, G., Sang, X.F., Shi, S., Wang, X.M., 2012. Levoglucosan and carbonaceous species in the background aerosol of coastal southeast China: case study on transport of biomass burning smoke from the Philippines. Environmental Science and Pollution Research 19, 244–255.

Zhang, Z.S., Engling, G., Chan, C.Y., Yang, Y.H., Lin, M., Shi, S., He, J., Li, Y.D., Wang, X.M., 2013. Determination of isoprene-derived secondary organic aerosol tracers (2-methyltetrols) by HPAEC-PAD: Results from size-resolved aerosols in a tropical rainforest. Atmospheric Environment 70, 468–476.

Zhao, S.Y., Tie, X.X., Long, X., Cao, J.J., 2017. Impacts of Himalayas on black carbon over the Tibetan Plateau during summer monsoon. Science of the Total Environment 598, 307–318.

Table 1. Average and standard deviation values for TSP, OC, EC, and biomass burning tracers (levoglucosan, mannosan, and galactosan) concentrations (μg m^{-3}) across winter, pre-monsoon, monsoon, and post-monsoon during November 2015 to November 2016.

	TSP	OC	EC	levoglucosan	mannosan	galactosan
Annual	15.2±6.4	2.1±0.64	0.74±0.22	0.097±0.051	0.023±0.012	0.004±0.003
Winter	16.7±4.4	2.1±0.44	0.87±0.24	0.131±0.073	0.028±0.019	0.007±0.004
Pre-monsoon	19.1±8.3	1.98±0.58	0.63±0.11	0.098±0.031	0.022±0.007	0.003±0.001
Monsoon	12.5±5.5	2.52±0.61	0.78±0.14	0.072±0.038	0.023±0.010	0.001±0.001
Post-monsoon	13.6±2.7	1.88±0.20	0.81±0.13	0.105±0.033	0.021±0.005	0.004±0.002

Figure Captions:

Figure 1. Geographic location of the sampling site, Lulang.

Figure 2. Temporal variability of TSP mass, OC, and EC (a), and variations of levoglucosan, mannosan, and galactosan for TSP (b).

Figure 3. Source profiles for TSP by PMF receptor model.

Figure 4. Time series of the % contribution from BB to the TSP OC and TSP mass at Lulang.

Figure 5. Scatter plots of PMF-derived BB TSP mass and BB TSP OC vs. levoglucosan and regression lines, forced through the origin.

Figure 6. Seasonal distributions of fire hot spots from the Terra and Aqua satellites during the sampling period.

Figure 7. The seasonal three-day air mass backward trajectories with levoglucosan concentrations using HYSPLIT model.

Figure 8. The four defined potential BB source distribution of PSCF using levoglucosan concentrations.

17

18

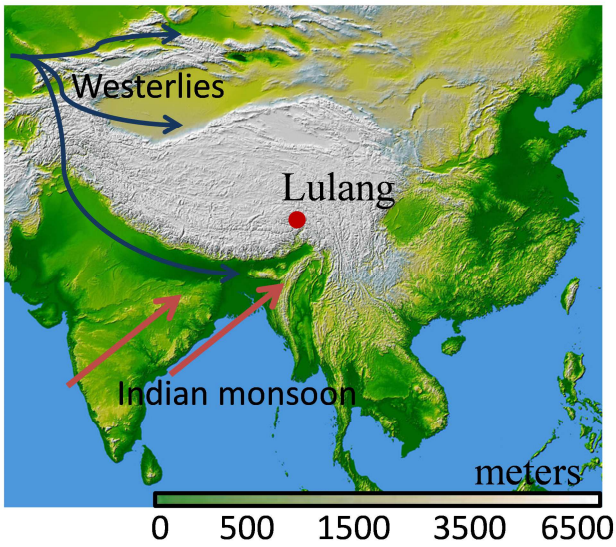

19

20 Figure 1

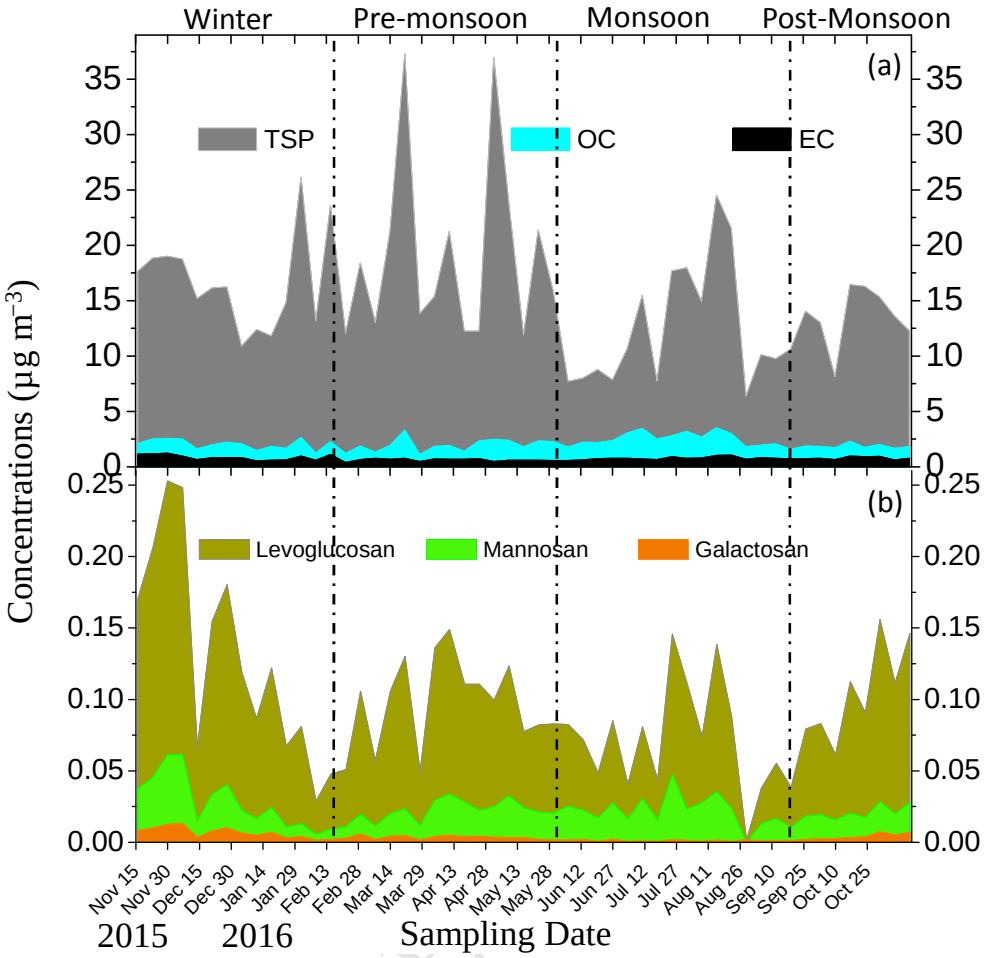

Figure 2.

Figure 3.

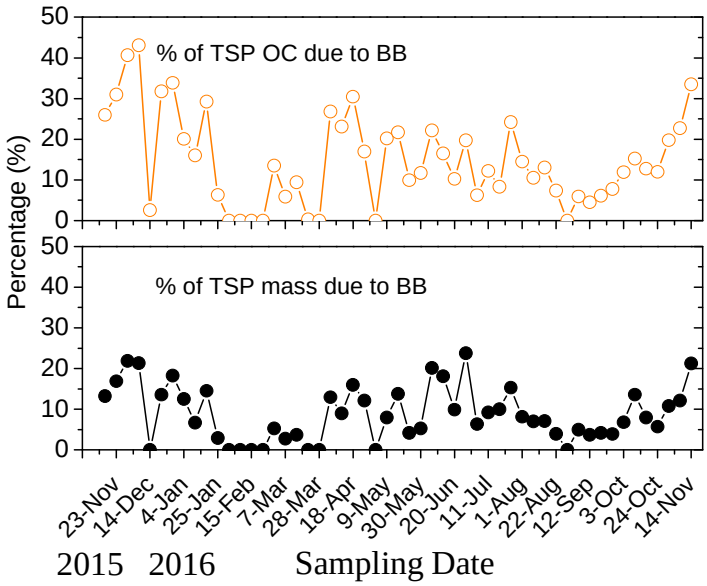

Figure 4.

39

40

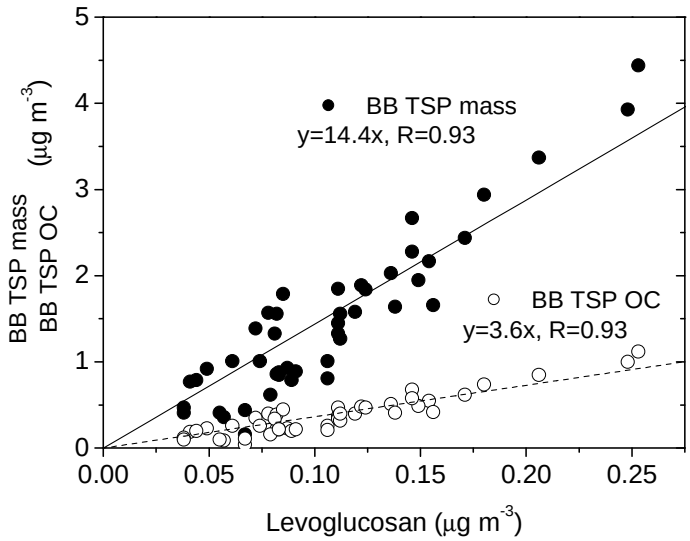

41

42 Figure 5

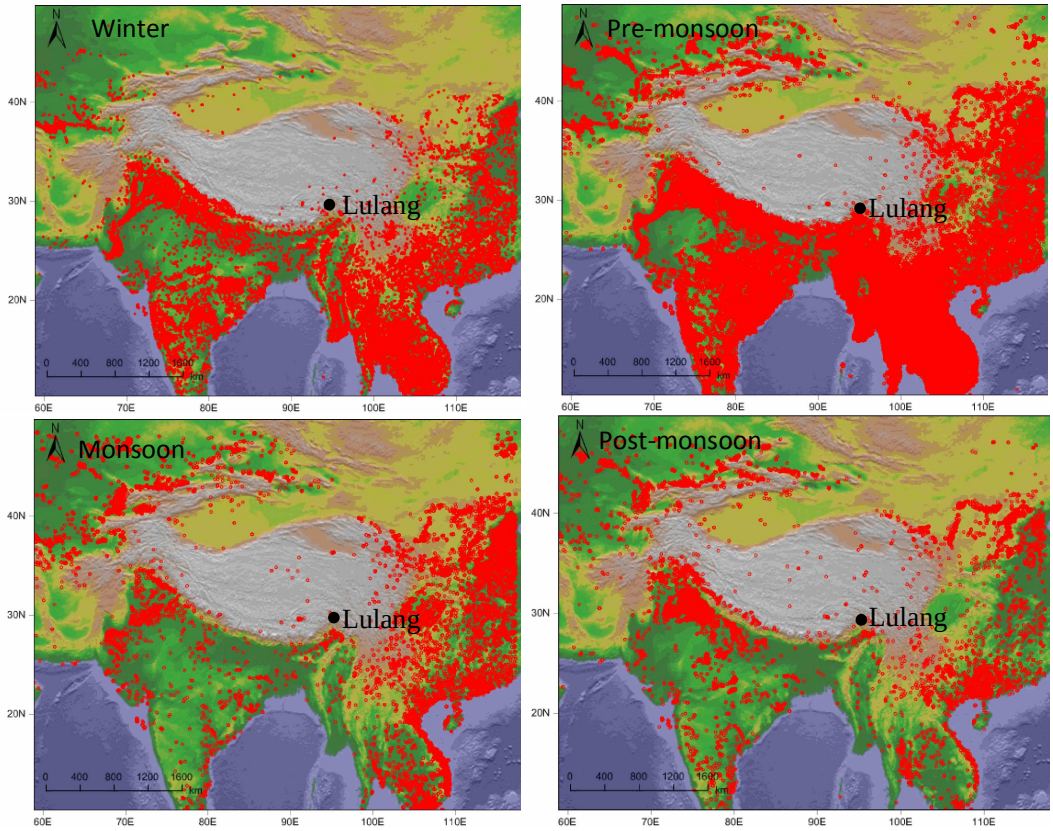

Figure 6

46

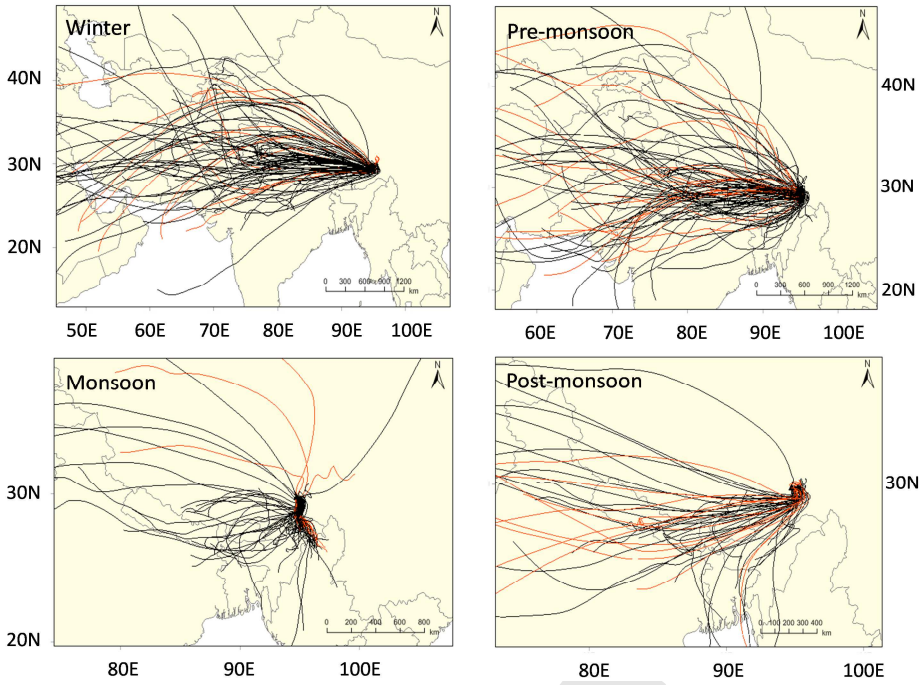

47

48 Figure 7

49

50

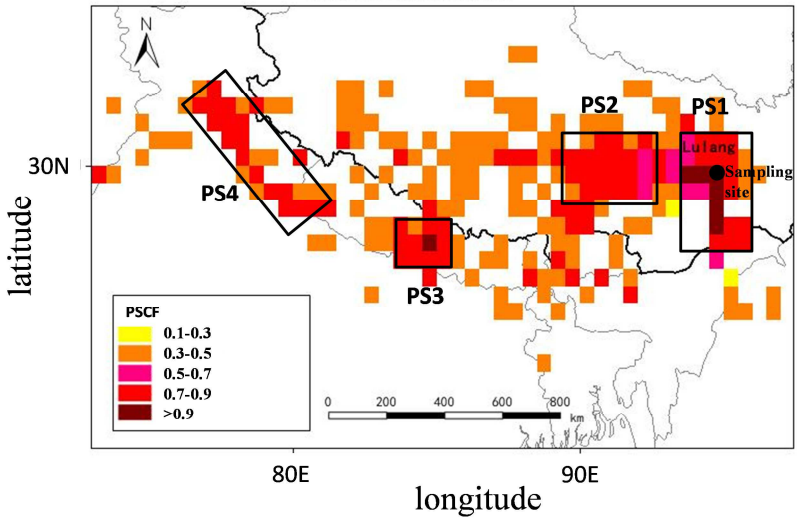

51

52 Figure 8

53

Highlights:

1. The variations of carbonaceous fractions and BB tracers were investigated at Lulang in the southeastern TP.
2. The contributions from BB to the TSP and OC mass indicated that BB is an important contributor in winter.
3. The BB pollutant transport and major potential source distributions were identified.